Joint 2-D angles and time delay estimation of coherent wideband signals

Xiangzhi Li*, *Weijia* Cui, *Haiyun* Xu, *Songtao* Yang, *Hao* Li, *Yankui* Zhang, *and Bin* Ba

National Digital Switching System Engineering & Technological Research Center, Zhengzhou, Henan Province (450001), China

Keywords: Joint DOA and TD estimation, Virtual spatial smoothing, Wideband signal.

Abstract. Joint direction of arrival (DOA) and time delay (TD) estimation of wideband signals such as WIFI and mobile communication signals has to face the challenges aroused by multipath effect in indoor environments. New methods that can deal with coherent wideband signals with high estimation accuracy are necessary. To achieve localization when signals are coherent, this paper proposes a new joint estimation method which fully utilizes the subcarriers of wideband signals. This method could greatly extend the array aperture and accomplish the joint estimation through UCA-ESPRIT and one-dimensional (1-D) search. Simulation experiments are conducted to show the validity and efficiency of this method.

1 Introduction

WIFI and mobile communication signals are typical wideband signals that have been widely applied in recent decades. As location-based services are becoming more and more popular, localization based on WIFI and mobile communication signals in indoor environments has a promising prospect [1]. These wideband signals utilize multi-carrier modulation (MCM) technology which contains more frequency points than traditional narrowband signals [2]. To achieve accurate localization, joint two-dimensional (2-D) angles and time delay (TD) estimation is considered by most of previous researchers. Especially in indoor environments where multipath effect is common, joint estimation methods that can deal with coherent signals are needed [3,4].

A number of methods have been proposed for joint estimation of DOA and TD. However, some of them cannot be used when signals are coherent [5]. While some others have too high computational complexity and poor estimation accuracy [6]. In this way, we propose a novel method for joint estimation in multipath environments based on UCA that can achieve both low computation and high accuracy. We first expand the virtual array aperture and obtain the extended array output. Then virtual spatial smoothing is deployed to eliminate the influence of multipath effect. Finally, UCA-ESPRIT and 1-D search are used to get the estimation results of DOA and TD. The estimation results show the performance of our proposed method.

* Corresponding author: lixiangzhi2231@163.com

2 Signal model

Consider a uniform circular array (UCA) consisting of M sensors with the radius r. There are P reflections of a far-field wideband signal $s(t)$ impinging on the array from directions $(\theta_p, \varphi_p), p = 1, 2, \cdots, P$, where φ_p is the angle between the direction of the p-th path and the x axis, while θ_p is the angle between the direction of the p-th path and the z axis, as is shown in Fig.1.

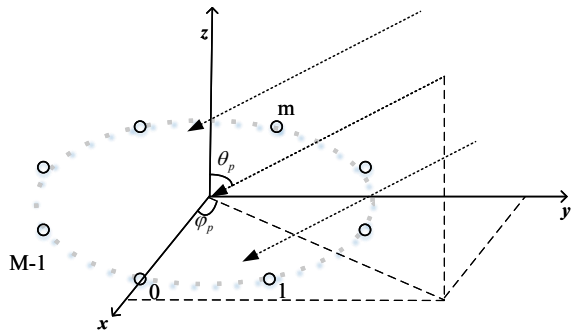

Fig. 1. UCA structure.

$\tau_p, p = 1, 2, \cdots, P$ is the time delay of the p-th path from the emission source to the center of the array. The array spatial responding vector is represented as

$$\mathbf{a}(\theta_p, \varphi_p) = \begin{bmatrix} a_1(\theta_p, \varphi_p) \\ a_2(\theta_p, \varphi_p) \\ \vdots \\ a_M(\theta_p, \varphi_p) \end{bmatrix} = \begin{bmatrix} e^{j2\pi r \sin(\theta_p)\cos(\varphi_p) f/c} \\ e^{j2\pi r \sin(\theta_p)\cos(\varphi_p - 2\pi/M) f/c} \\ \vdots \\ e^{j2\pi r \sin(\theta_p)\cos(\varphi_p + 2\pi/M) f/c} \end{bmatrix}, \quad (1)$$

where c is the speed of light and f is the frequency. Though there are different f in the wideband signal, the change of f/c is extremely small and negligible. For the clarity of processing, all frequencies of $s(t)$ are approximated to f. The received data of m-th sensor at time t_n could be represented as

$$x_m(t_n) = \sum_{p=1}^{P} \alpha_p e^{j\beta_p} a_m(\theta_p, \varphi_p) s(t_n - \tau_p) + n_m(t_n), \quad (2)$$

where $\alpha_p e^{j\beta_p}$ is the complex attenuation of p-th path, α_p is the amplitude, and β_p is the phase with a uniform distribution represented as $\beta_p \sim U(0, 2\pi)$; they are both independent on the change of t. $n(t) \sim N(0, \sigma^2)$ is additive white Gaussian noise which is independent from

the signal. The complex signal $s(t)$ is known. Then the output of the array could be expressed as

$$\mathbf{x}(t_n)=\sum_{p=1}^{P}\alpha_p e^{j\beta_p}\mathbf{a}(\theta_p,\varphi_p)s(t_n-\tau_p)+\mathbf{n}(t_n) \quad , \tag{3}$$

where $\mathbf{x}(t_n)=\left[x_1(t_n)\quad x_2(t_n)\quad\cdots\quad x_M(t_n)\right]^{\mathrm{T}}$, an $\mathbf{n}(t_n)=\left[n_1(t_n)\quad n_2(t_n)\quad\cdots\quad n_M(t_n)\right]^{\mathrm{T}}$. Then assume there are L subcarriers, the received signal of m -th sensor at l -th subcarrier f_l in frequency domain could be modeled as

$$X_m(f_l)=\sum_{p=1}^{P}\alpha_p e^{j\beta_p}a_m(\theta_p,\varphi_p)S(f_l)e^{-j2\pi f_l\tau_p}+N_m(f_l) \quad , \tag{4}$$

where $X_m(f_l)$, $S(f_l)$, and $N_m(f_l)$ are the discrete Fourier transform (DFT) of $x_m(t_n)$, $s(t_n)$, and $n_m(t_n)$ respectively. $f_l=f+(l-1)\Delta f, l=1,2,\cdots,L$. Similarly, the frequency-domain expression of Eq. 3 is

$$\begin{aligned}\mathbf{X}(f_l)&=\sum_{p=1}^{P}\alpha_p e^{j\beta_p}\mathbf{a}(\theta_p,\varphi_p)S(f_l)e^{-j2\pi f_l\tau_p}+\mathbf{N}(f_l)\\&=\mathbf{A}_l\mathbf{B}S(f_l)+\mathbf{N}(f_l)\end{aligned} \quad , \tag{5}$$

where

$$\mathbf{A}_l=\left[\mathbf{a}(\theta_1,\varphi_1)\kappa_1^{\,l-1}\quad \mathbf{a}(\theta_2,\varphi_2)\kappa_2^{\,l-1}\quad\cdots\quad \mathbf{a}(\theta_P,\varphi_P)\kappa_P^{\,l-1}\right], \tag{6}$$

$$\mathbf{B}=\left[\alpha_1 e^{j\beta_1}e^{-j2\pi f\tau_1}\quad \alpha_2 e^{j\beta_2}e^{-j2\pi f\tau_2}\quad\cdots\quad \alpha_P e^{j\beta_P}e^{-j2\pi f\tau_P}\right]^{\mathrm{T}}, \tag{7}$$

$$\kappa_p=e^{-j2\pi\Delta f\tau_p} \tag{8}$$

Since the frequency-domain incident signal $S(f_l), l=1,2,\cdots,L$ could be got, Eq. 5 could be expressed as

$$\mathbf{X}(f_l)=\frac{S(f_l)}{S}\mathbf{A}_l\mathbf{B}S+\mathbf{N}(f_l)=\mu_l\mathbf{A}_l\mathbf{B}S+\mathbf{N}(f_l) \quad , \tag{9}$$

where S is the statistical average value of $S(f_l), l=1,2,\cdots,L$, written as

$$S = \frac{1}{L}\sum_{l=1}^{L} S(f_l) \quad . \tag{10}$$

Then the extended array output which contains all subcarriers could be expressed as

$$\mathbf{X} = \begin{bmatrix} \mathbf{X}(f_1) \\ \mathbf{X}(f_2) \\ \vdots \\ \mathbf{X}(f_L) \end{bmatrix} = \begin{bmatrix} \mu_1\mathbf{A}_1 \\ \mu_2\mathbf{A}_2 \\ \vdots \\ \mu_L\mathbf{A}_L \end{bmatrix} \mathbf{B}S + \begin{bmatrix} \mathbf{N}(f_1) \\ \mathbf{N}(f_2) \\ \vdots \\ \mathbf{N}(f_L) \end{bmatrix} = \mathbf{AB}S + \mathbf{N} \quad , \tag{11}$$

where $\mathbf{A}$ is the reconstructed manifold matrix which contains DOA and TD information of all the L paths; $\mathbf{N}$ is the noise matrix.

The uniformly distributed subcarriers are used to expand the dimension of the manifold matrix $\mathbf{A}$ in frequency domain, functioning the same as the spatially distributed sensors. As can be seen from Eq. 11, $\mathbf{A}$ is a $ML \times P$ matrix, which means that the number of virtual array elements is ML, so the array aperture is greatly expanded.

3 Joint estimation method

For this section, we'll introduce the proposed estimation method. Generally, the covariance matrix $\mathbf{R_X}$ of the extended array output $\mathbf{X}$ is required in joint estimation, which could be expressed as

$$\mathbf{R_X} = E\left[\mathbf{XX}^{\mathrm{H}}\right] = \mathbf{AR_B A}^{\mathrm{H}} + \sigma^2\mathbf{I} \quad . \tag{12}$$

In Eq. 12, $\mathbf{R_B}$ is the covariance matrix of complex attenuation matrix $\mathbf{B}S$.

When the paths are independent, it would be clear that $rank(\mathbf{R_B}) = P$. As $\mathbf{A}$ is of full column rank, we can get $rank(\mathbf{R_X}) = P$. In this way, the MUSIC algorithm, one of subspace-based methods, could be used to estimate the parameters. However, when the channels are coherent, the rank of the covariance matrix is 1. In this case, the accuracy of methods based on eigen decomposition cannot be ensured and there will be interference in the estimation results of different paths. In this way, the multipath effect needs to be solved and spatial smoothing is one typical solution.

3.1 Virtual spatial smoothing

Smoothing processing is adopted when the rank of covariance matrix is smaller than the number of paths to estimate. Generally, the array will be divided into several subarrays that have the same structure. By making full use of the relationship between adjacent sub-array manifold matrices, the negative impact of multipath effect on the estimation could be greatly eliminated.

In this paper, the extended manifold matrix $\mathbf{A}$ is divided into L sub-array matrices, which are $\mu_l\mathbf{A}_l, l = 1, 2, \cdots, L$. That is to say, the l-th virtual sub-array contains the information of all sensors received from the l-th subcarrier.

We first calculate the covariance matrix of each sub-array. Assume the covariance matrix of the l -th subcarrier is R_l , then we have

$$\mathbf{R}_l = E\left[\mathbf{X}_l\mathbf{X}_l^{\mathrm{H}}\right] = \left|\mu_l\right|^2 \mathbf{A}_l\mathbf{R}_\mathbf{B}\mathbf{A}_l^{\mathrm{H}} + \sigma^2\mathbf{I} \quad . \tag{13}$$

According to Eq. 6, it could be got that

$$\mathbf{A}_{l+1} = \mathbf{A}_l\mathbf{D} \quad , \tag{14}$$

where $\mathbf{D} = diag\left(\kappa_1 \quad \kappa_2 \quad \cdots \quad \kappa_P\right)$, so $\mathbf{R}_{l+1}$ could be expressed as

$$\begin{aligned}\mathbf{R}_{l+1} &= \left|\mu_{l+1}\right|^2 \mathbf{A}_{l+1}\mathbf{R}_\mathbf{B}\mathbf{A}_{l+1}^{\mathrm{H}} + \sigma^2\mathbf{I} \\ &= \left|\mu_{l+1}\right|^2 \mathbf{A}_l\mathbf{D}\mathbf{R}_\mathbf{B}\mathbf{D}\mathbf{A}_l^{\mathrm{H}} + \sigma^2\mathbf{I} \quad .\end{aligned} \tag{15}$$

The key step of virtual spatial smoothing is calculating the mean of $\mathbf{R}_l, l = 1, 2, \cdots, L$ to get a full-rank covariance matrix, which is given as

$$\begin{aligned}\tilde{\mathbf{R}} &= \frac{1}{L}\sum_{l=1}^{L}\mathbf{R}_l \\ &= \mathbf{A}_1\left(\frac{1}{L}\sum_{l=1}^{L}\left|\mu_l\right|^2 \mathbf{D}^{l-1}\mathbf{R}_\mathbf{B}\left(\mathbf{D}^{l-1}\right)^{\mathrm{H}}\right)\mathbf{A}_1^{\mathrm{H}} + \sigma^2\mathbf{I} \\ &= \mathbf{A}_1\tilde{\mathbf{R}}_\mathbf{B}\mathbf{A}_1^{\mathrm{H}} + \sigma^2\mathbf{I} \quad ,\end{aligned} \tag{16}$$

where $\tilde{\mathbf{R}}_\mathbf{B} = \frac{1}{L}\sum_{l=1}^{L}\left|\mu_l\right|^2 \mathbf{D}^{l-1}\mathbf{R}_\mathbf{B}\left(\mathbf{D}^{l-1}\right)^{\mathrm{H}}$.

3.2 UCA-ESPRIT for DOA estimation

The next step of the proposed joint estimation method is DOA estimation using UCA-ESPRIT. UCA-ESPRIT is an improved ESPRIT method designed for uniform circular arrays because the array manifold of UCAs is not a Vandermonde matrix, leading to the lack of rotational invariance. In this way, the technology of beam-space transformation is deployed to process the data received by UCAs.

Assume $\mathbf{F}^{\mathrm{H}}$ is the beam-space transform matrix, and $\tilde{\mathbf{S}}$ is signal space after the beam-space transformation. Then we have

$$\tilde{\mathbf{S}} = \mathbf{F}^{\mathrm{H}}\mathbf{A}_1\mathbf{Q} \quad , \tag{17}$$

where $\mathbf{Q}$ is a $P \times P$ full rank matrix. Next, define

$$\tilde{\mathbf{S}}' = \mathbf{C}_0\mathbf{W}\tilde{\mathbf{S}} \quad , \tag{18}$$

where $\mathbf{C}_0 = diag\left\{(-1)^M \quad \cdots \quad (-1)^1 \quad 1 \quad \cdots \quad 1^M\right\}$,
$\mathbf{W} = \frac{1}{\sqrt{M}}\left[\mathbf{v}(\gamma_{-M}) \quad \cdots \quad \mathbf{v}(\gamma_0) \quad \cdots \quad \mathbf{v}(\gamma_M)\right]$, $\mathbf{v}(x) = \left[e^{-jMx} \quad \cdots \quad e^{j0x} \quad \cdots \quad e^{jMx}\right]^{\mathrm{T}}$, and $\gamma_m = \frac{2\pi m}{M}$.

$\tilde{\mathbf{S}}'$ could be divided into three matrices from top to the bottom, $\tilde{\mathbf{S}}'_t$, $\tilde{\mathbf{S}}'_m$, $\tilde{\mathbf{S}}'_b$, each of which has $2M-1$ rows. It could be obtained that

$$\mathbf{E}\bar{\mathbf{\Psi}} = \mathbf{\Gamma}\tilde{\mathbf{S}}'_m, \tag{19}$$

where $\mathbf{\Gamma} = \frac{\lambda}{\pi r} diag\left\{-(M-1) \quad \cdots \quad 0 \quad \cdots \quad M-1\right\}$, $\mathbf{E} = \left[\tilde{\mathbf{S}}'_t \quad \tilde{\mathbf{S}}'_b\right]$, and $\bar{\mathbf{\Psi}} = \left[\mathbf{\Psi}^{\mathrm{T}} \quad \mathbf{\Psi}^{\mathrm{H}}\right]$. $\mathbf{\Psi}$ could be expressed as $\mathbf{\Psi} = \mathbf{Q}^{-1}\mathbf{\Phi}\mathbf{Q}$, and

$$\mathbf{\Phi} = diag\left(\sin\theta_1 e^{j\varphi_1} \quad \sin\theta_2 e^{j\varphi_2} \quad \cdots \quad \sin\theta_P e^{j\varphi_P}\right). \tag{20}$$

Then take the eigenvalue decomposition of $\mathbf{\Phi}$ and get its eigenvalue $\lambda_p, p = 1, 2, \cdots, P$. The closed-from solutions of DOA are

$$\hat{\theta}_p = \arcsin\left(\left|\lambda_p\right|\right), \hat{\varphi}_p = angle\left(\lambda_p\right). \tag{21}$$

3.3 1-D search for time delay estimation

Based on the estimation results of DOA obtained through UCA-ESPRIT, we then use one-dimensional (1-D) research method to estimate time delays, the spatial spectrum function could be expressed as

$$P(\tau) = \frac{1}{\mathbf{a}_1^{\mathrm{H}}\left(\tau, \hat{\theta}_p, \hat{\varphi}_p\right)\tilde{\mathbf{U}}_N\tilde{\mathbf{U}}_N^{\mathrm{H}}\mathbf{a}_1\left(\tau, \hat{\theta}_p, \hat{\varphi}_p\right)}, p = 1, 2, \cdots, P. \tag{22}$$

We can get corresponding estimation result $\hat{\tau}_p$ for each $\left(\hat{\theta}_p, \hat{\varphi}_p\right)$. In this way, joint estimation of DOA and time delay is accomplished.

4 Simulation results

In this section, we conduct two simulation experiments to examine the validity and accuracy of the proposed method. We consider a wideband signal with $f = 2.4\text{GHz}$, $L = 64$ subcarriers, guard duration 1.6μs, fast Fourier transform period 3.2μs, and bandwidth 80MHz. The UCA has $M = 15$ sensors. For three coherent signals, elevation angles are [20°,30°,45°], azimuth angles are [-20°,0°,30°], and time delays are [3.5*ns*,13.5*ns*,23.5*ns*], respectively.

In the first simulation, the performance of this method under low signal-to-noise ratio (SNR) condition is examined. With 200 Monte Carlo simulations, the estimation results distribution is shown in Fig.2 and Fig.3.

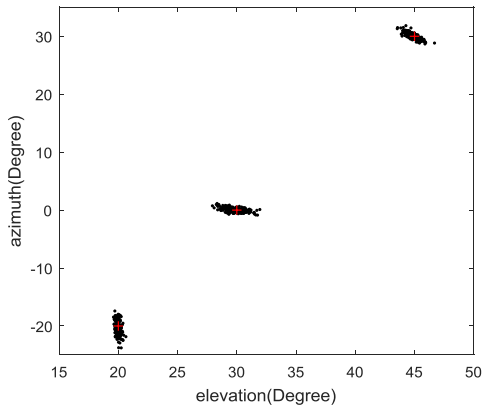

Fig. 2. Estimation results distribution of elevation and azimuth angles when SNR=-5Db.

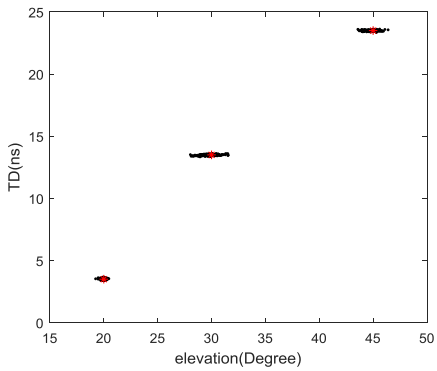

Fig. 3. Estimation results distribution of elevation angle and time delay when SNR=-5dB.

It can be seen from the above figures that the estimation results are all concentrated in the true values, which indicates the effectiveness and validity of our method when dealing with coherent signals under low SNR.

The second simulation is conducted to evaluate the performance of the method proposed in this paper. We choose root mean square error (RMSE) as the measure index, which is defined as

$$RMSE = \sqrt{\frac{1}{Q}\sum_{i=1}^{Q}\left\|x-\hat{x}_i\right\|^2}, \tag{23}$$

where $Q = 200$ is the number of Monte Carlo simulations, x and $\hat{x}_i$ are the true value and the i -th estimation value. SNR in this simulation ranges from -15dB to 20dB at 5dB intervals. The estimation performance of our method and the approximate maximun likelihood (AML) algorithm in [6] is shown in Fig.4 and Fig.5.

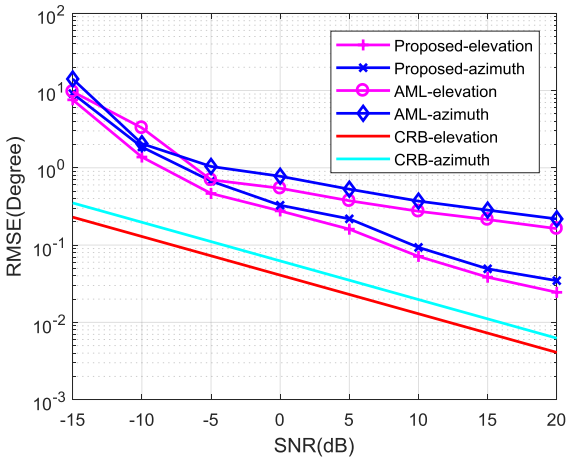

Fig. 4. Performance of DOA.

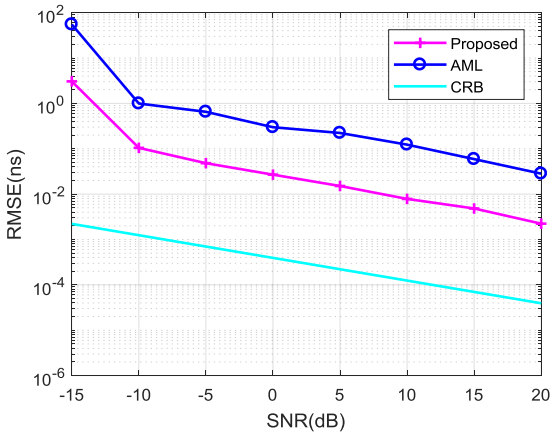

Fig. 5. Performance of TD.

It is evident that the proposed method is more accurate than the AML method and is more close to the CRB. Consequently, our method is more efficient when dealing with coherent signals.

5 Conclusion

For wideband signals in indoor environments, this paper proposes a novel joint DOA and TD estimation method that can deal with coherent signals. The virtual array aperture is greatly expanded by dividing wideband signals into several subcarriers. After virtual spatial smoothing processing, the joint estimation is accomplished by using UCA-ESPRIT and 1-D search method. Simulation results show that the proposed method has good performance under low SNR conditions and brings better estimation accuracy than typical AML algorithm.

This research was financially supported by Grant No.61401513 from the National Science Foundation.

References

1. Y. Rezgui, L. Pei, X. Chen, F. Wen, and C. Han. An efficient normalized rank-based SVM for room level indoor WiFi localization with diverse devices, J. Mobile Information Systems 2017(2017):1-19.
2. Z. Mokhtari, M. Sabbaghian, R. Dinis. A Survey on Massive MIMO Systems in Presence of Channel and Hardware Impairments, J. Sensors 19.1 (2019): 164.
3. H. Xu, Y. Zhang, B. Ba, D. Wang, and X. Li. Fast joint estimation of time of arrival and angle of arrival in complex multipath environment using OFDM, J. IEEE Access 6 (2018): 60613-60621.
4. L. Chen, W. Qi, E. Yuan, and Y. Zhao. Joint 2-D DOA and TOA estimation for multipath OFDM signals based on three antennas, J. IEEE Communications Letters. 22.2 (2017): 324-327.
5. B. Ba, G. Liu, et al. Joint for time of arrival and direction of arrival estimation algorithm based on the subspace of extended hadamard product, J. Acta Physica Sinica -Chinese Edition- 64.7(2015):78403-078403.
6. F Wen, P Liu, H Wei, Y Zhang. Joint Azimuth, Elevation, and Delay Estimation for 3-D Indoor Localization, J. IEEE Transactions on Vehicular Technology 67.5 (2018): 4248-4261.